Extended Abstracts of the 2007 International Conference on Solid State Devices and Materials, Tsukuba, 2007, pp. 272-273

D-3-3

A New Symmetric Inductor Model for RF Circuits under Single-end and Differential Operations

Jyh-Chyurn Guo and **Teng-Yang Tan**
E-mail: jcguo@mail.nctu.edu.tw, Tel : 886-3-5131368, Fax : 886-3-5724361
Institute of Electronics, National Chiao-Tung University, 1001 Ta-Hsueh Rd, Hsinchu, 30010 Taiwan, R.O.C.

ABSTRACT— A broadband and scalable 2-T model is developed to accurately simulate fully symmetric inductor with various dimensions. A single set of model parameters can fit both single-end and differentially driven topologies. The broadband accuracy is proven by good match with S-parameters, L(ω), Re(Z_{in}(ω)), and Q(ω) over frequencies up to 20 GHz. The scalability is justified by good fitting with either a linear or a parabolic function of spiral coil radii. This 2-T model consistently predicts Q_{max} enhancement by 20~30% and more than 100% Q improvement over broader bandwidth beyond $f_m(Q_{max})$ for the symmetric inductors under differential excitation.

I. Introduction

On-chip symmetric inductors become increasingly important for low noise and low power RF circuit design. [1-2]. Given VCO design as an example, the adoption of differential inductors can realize lower phase noise due to higher Q, larger tuning range attributed to higher f_{SR}, and saving of single-end to differential conversion circuitry for the LO drive in a Gilbert-cell mixer [2-3]. Unfortunately, the conventional differential inductors are not truly symmetric in geometry and structure [4]. A fully symmetric inductor with new layout was proposed to improve the symmetry in 2-port S-parameters [4]. However, degraded Q compared with the conventional ones appears as a weakness to be solved. The requirement of an accurate and computation efficient model to fit both single-end and differential operations emerges as another challenge for RF circuit simulation and design. A lumped element equivalent circuit model with Spice compatible efficiency was proposed [5]. However, different model parameters required for single-end and differential topologies suggest themselves unphysical and incur difficulty in prediction. Furthermore, the scalability to fit various geometries was not verified and demonstrated.

In this paper, a 2-T model is developed as a successful extension of our original T-model for spiral inductors [6]. This 2-T model can realize the features of broadband accuracy and scalability. A new parameter extraction method was established through equivalent circuit analysis under differential and single-end excitations. The differential excitation can drive the on-chip inductor free from substrate loss and simplify the parameter extraction. A single set of model parameters can fit both single-end and differentially driven topologies. All model parameters are frequency independent to be easily deployed in a circuit simulator.

II. Symmetric Inductor Structures and Technology

A new fully symmetric inductor was fabricated by 0.13μm BEOL technology. The top metal of 3μm Cu was used to implement the spiral coils. Fig.1 illustrates layout of the new symmetric inductor in which taper structure with varying metal trace widths is the major enhancement over the original one [4] to solve the weakness of degraded Q. The inter-trace space was fixed at 2 μm and inner radii of R=30, 60, and 90 μm were splits for scalability verification. The physical inductances achieved at sufficiently low frequency are around 0.6~1.9 nH corresponding to R=30~90 μm.

III. 2-T Model Equivalent Circuit & Parameter Extraction

Fig.2(a) illustrates the equivalent circuit of 2-T model proposed for on-chip fully symmetric inductors. A pair of identical RLC networks represents the symmetric spiral coils and a substrate RLC network is shared by the pair of spiral coils. The capacitances $C_{ox,1,2,3}$ deployed between the coil and substrate networks account for the coupling between the spiral inductors and lossy substrate underneath. A pair of series R_{sk} and L_{sk} is used to simulate proximity effect, which is originated from augmented EM coupling between two closely placed spiral coils.

The original circuit schematics can be mapped to the topologies consisting of $Z_{dut1,2}$ $Z_{ox1,2,3}$, and Z_{sub} shown in Figs.2(b) and (c) corresponding to differential and single-end excitations. This 2-T model as an extension of our original T-model for single-end spiral inductor [6] is targeted to fit the symmetric inductor under single-end and differentially driven operations. For differential excitation with two port signals being 180° out of phase, Z_{sub} and Z_{ox3} can be neglected and then the differential input impedance Z_d is simplified to a parallel combination of (Z_{dut1}+Z_{dut2}) and (Z_{ox1}+Z_{ox2}) shown in Fig.2(b). This simplified circuit topology helps reduce the extraction flow and enable extraction of spiral coil network elements. As for single-end excitation, the existence of Z_{sub} and Z_{ox3} in Fig.2(c) makes the circuit analysis more sophisticated. Circuit transformation from Fig.2(c) to (d) is done and followed by π-to-T topology conversion to extract the substrate network parameters. Based on the circuit topology conversion and analysis, the model parameters can be extracted. Fig.3 draws a complete extraction flow with detailed formulas for extracting all the model parameters.

IV. 2-T Model Broadband Accuracy and Scalability

Figs.4(a)~(d) indicate good agreement between the 2-T model and measurement for S_{11} and S_{21} associated with various coil radii. More extensive verification has been done through comparison of L(ω) (=Im(Z_{in}(ω)/ω), Re(Z_{in}(ω)), and Q(ω). Q(ω) is the quality factor defined by ωL(ω)/Re(Z_{in}(ω). Figs.5 illustrate the excellent fit to the measured L(ω) and Re(Z_{in}(ω)) under single-end excitation for all inductors operating to 20GHz. The transition from inductive to capacitive mode at f > f_{SR} is accurately reproduced for the largest inductor (f_{SR}=16 GHz for R=90 μm).

Regarding the differential excitation, 2-T model accuracy is certified by good agreement with measurement in terms of Re(S_d), Im(S_d), Re(Z_d), and Im(Z_d) shown in Figs.6(a)-(d). Q(ω) is the most critical parameter governing RF IC performance like power, gain, and noise. Figs.7(a) and (b) demonstrate promisingly good match with the measured Q(ω) for both singled-end and differential topologies (Q_{se}, Q_d) over broadband of 20 GHz. In Figs.7(c) and (d), the comparison between Q_{se} and Q_d reveals Q_{max} improvement of around 20~30% by Q_d w.r.t. Q_{se} and more than 100% Q improvement over broader bandwidth beyond $f_m(Q_{max})$. As a result, it is proven that a single set of model parameters can fit both single-end and differential topologies.

Another important feature is the good scalability w.r.t. dimension for all model parameters. Figs.8 present all model parameters in the spiral coil network (R_s, L_s, R_p, C_p, R_{sk}, L_{sk}), and C_{ox} under varying coil radii. All the elements except L_{sk} increase with the coil radius (R) following a linear function. Interestingly, L_{sk} decreases according to a parabolic function of R. The larger L_{sk} associated with the smaller R suggests that the smaller inductors with smaller coil radii may suffer worse proximity effect due to the magnetic field coupling of the closely placed coils in the fully symmetric inductor. Figs.9 indicate the excellent fit by linear functions for substrate network parameters, C_{sub}, 1/R_{sub}, L_{sub}, and R_{loss}. The proven scalability suggests that this 2-T model can be used for pre-layout simulation and optimization.

V. Conclusion

A broadband and scalable 2-T model has been developed for accurate simulation of on-chip fully symmetric inductors. A single set of model parameters can fit both single-ended and differential operations. The broadband accuracy is proven by S-parameters, L(ω), Re(Z_{in}), and Q(ω) over frequencies up to 20 GHz. The scalability is justified by good fitting with either a linear or a parabolic function of coil radii. This 2-T model consistently predicts Q_{max} enhancement by 20~30% and much broader operating bandwidth for differential excitation. The scalable model can facilitate optimization design of symmetric inductors through model parameters relevant to various geometries. Besides, the broadband accuracy proven by both single-end and differential excitations is useful for widely used differential topologies and broadband RF IC design.

Acknowledgement : The authors acknowledge the support from NSC 95-2221-E009-289, NDL CiC and RF Lab.

References

[1] *Tser-Yu Lin*, et al., in 2003 ISCAS Proc., pp.641-644
[2] *M. Tiebout*, IEEE JSSC vol.36, pp.1018-1024, July 2001
[3] *R. L. Bunch*, et al., IEEE Microwave Magzine, pp.82-92, June, 2002
[4] *J.-H. Gau*, et al., IEEE EDL vol.25, pp.608-609, Sept. 2004
[5] *M. Danesh*, et al., IEEE T-MTT vol.50, pp. 332-341, Jan. 2002
[6] *Jyh-Chyurn Guo*, et al., IEEE TED, vol. 53, pp.413-421, Mar. 2006

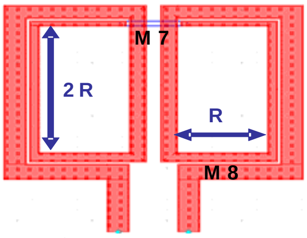

Fig.1 The layout of a new fully symmetric inductor with taper structure of varying metal trace widths (5~15μm)

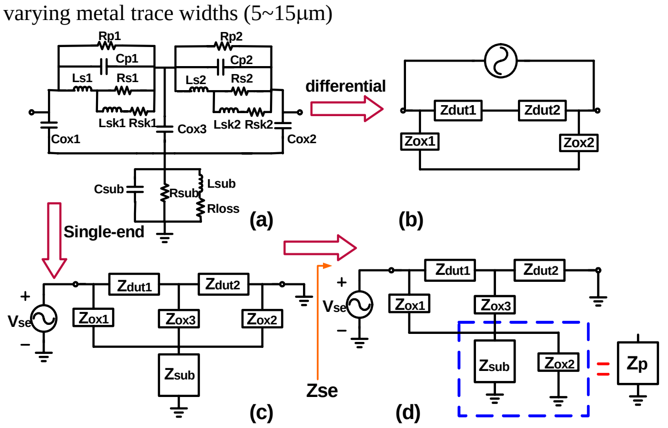

Fig.2 2T-model (a) original equivalent circuit schematics (b) reduced circuit block under differential excitation (c) circuit block under single-end excitation (d) transformation from (c) for model parameter extraction

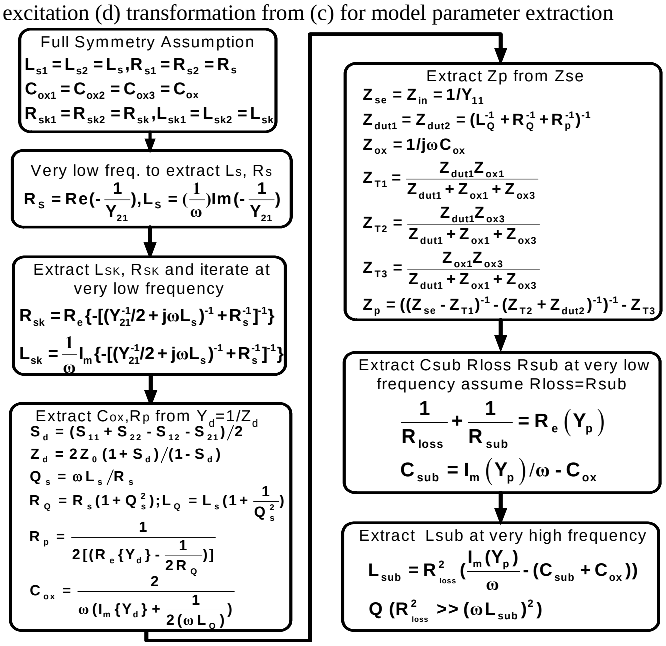

Fig.3 2-T-model parameter extraction flow with formulas

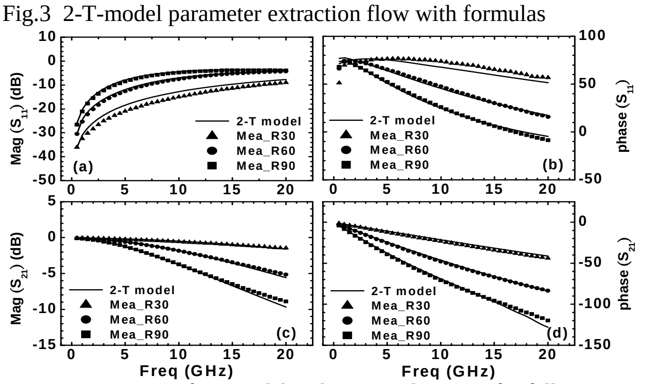

Fig. 4 Comparison of 2T-model and measured S_{11}, S_{21} for fully symmetric inductors with various R (30,60,90μm) (a) mag(S_{11}) (b) phase(S_{11}) (c) mag(S_{21}) (a) phase(S_{21}).

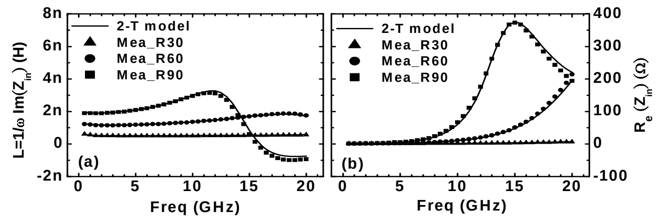

Fig. 5 Comparison of 2T-model and measurement for fully symmetric inductors under single-end excitation (a) $L(\omega)=Im(Z_{in}(\omega))/\omega$ (b) $Re(Z_{in}(\omega))$

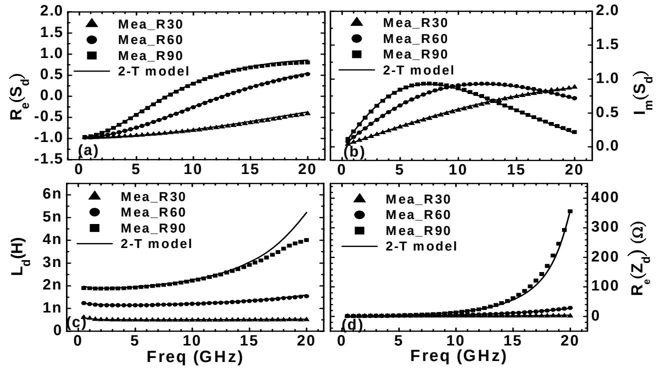

Fig. 6 Comparison of 2T-model and measurement for fully symmetric inductors under differential excitation (a) $Re(S_d)$ (b) $Im(S_d)$ (c) $L_d=Im(Z_d)/\omega$ (b) $Re(Z_d)$

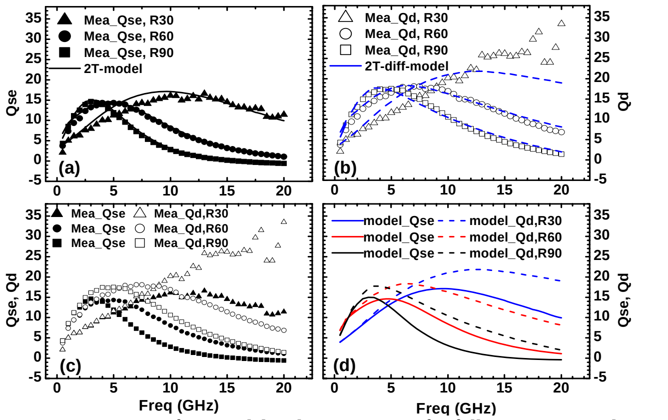

Fig. 7 Comparison of 2T-model and measurement for fully symmetric inductors (a)Q_{se} (b) Q_d, comparison of Q_{se} and Q_d (c) measure (d) 2T model

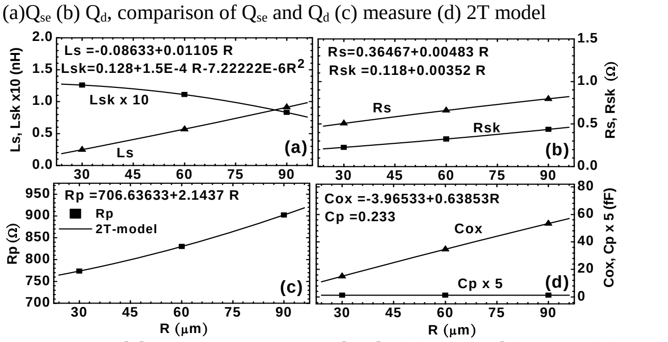

Fig. 8 2T model parameters versus coil radii (a) L_S, L_{sk} (b) R_S, R_{sk} (c) R_P (d) C_{ox}, C_P in the spiral coil network

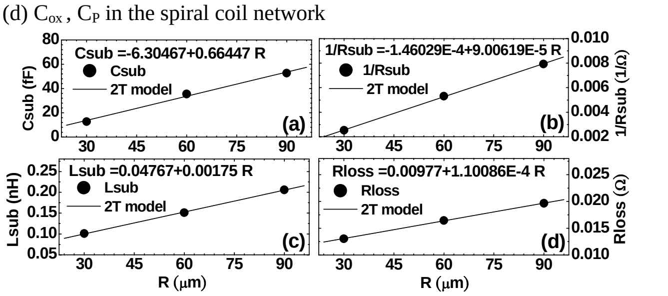

Fig. 9 2T model parameters versus coil radii (a) C_{sub} (b) $1/R_{sub}$ (c) L_{sub} (d) R_{loss} in the substrate network